An Improved Image Retrieval by Using Texture Color Descriptor with Novel Local Textural Patterns

Punit Kumar Johari[1], Rajendra Kumar Gupta[2]
Department of CSE and IT
Madhav Institute of Technology and Science, Gwalior, India

***Abstract*—This paper proposes a new local descriptor of color, texture known as a Median Binary Pattern for color images (MBPC) and Median Binary Pattern of the Hue (MBPH). These suggested methods are extract discriminative features for the color image retrieval. In the surrounding region of a local window, the suggested descriptor classification uses a plane to a threshold that distinguish two classes of color pixels. The Median Binary Patterns of the hue features are derived in the color space from HIS, called MBPH to maximize the discriminatory power of the proposed MBPC operator. In addition to MBPC, MBPH are fused to extract the MBPC+MBPH resulting in an efficient image recovery method combined with color histogram (CH). The structure of the two suggested MBPC and MBPH descriptors are combined with the other fuzzyfied based color histogram descriptor that formed MBPC+MBPH+FCH to improve the performance of the suggested method. The proposed methods are applied on datasets Wang, Corel-5K, and Corel-10K. Experimental results depicted that results of proposed methods are better than existing method in terms of retrieved accuracy. The significant recognition accuracy obtained from the proposed methods which is 60.1 and 63.9 for Wang dataset, 41.88 and 42.47 for Corel-5K and 32.89 and 33.89 for Corel-10K dataset. This hybrid proposed method greatly deals with different textural patterns as well as able to grasp minute color details.**

Keywords*—Image retrieval; Binary pattern; feature extraction; Median Binary Pattern for Color (MBPC) image; Median Binary Pattern for Hue (MBPH)

I. INTRODUCTION

One of the demanding research domain in the context of intelligent system and computer vision is Content Based Image Retrieval (CBIR). In the past, with the explosion of digital technologies such as multimedia sharing platforms, social networks, and priceless technology available with at most every people that produces millions of images in different scenario and replicate via hosting services [1, 2].

The relevant information is possible only with searching and indexing the massive volume of accessible digital images [3, 4] is only possible with more-and-more likely information retrieval system. Now a days at the advancement of the research domains the CBIR system has paying attention towards various researchers to improve methods which gives high recovery proportion inside less recovery rate. In the last decade, CBIR frameworks were boosted on the grayscale images, at that point by methods for the broad utilization of color image over the various systems, that improvement of a color characteristics for acknowledgement and getting reason. Now it is being joined to upgrade the recovery framework execution. Therefore, designing precise and fast system has become demanding research domain in the field of recognition of pattern and AI. The CBIR system mainly work on two criteria: extraction of feature and matching feature. The key criteria is feature extraction as it requires with very small variation to be signified by vastly discriminated features from the image. These features discriminate within the class images and major variations between the other existing class images. Essentially building block of the CBIR framework gets request image as input from the expected user and for the purpose of feature extraction from the query image it utilizes a descriptor (may be combination of image content) [5,6]. Different indexing methods has been utilized and the query image highlights is contrasted and the arrangement of highlight vectors of various picture database. The retrieval of images based on most related images from an image database and delivered to the user.

Mainly researchers are focused the features extraction procedures according to the application requirement in different domains. The main goal is to extract distinct features in the viable time. Features extraction is an important task for any multimedia retrieval process. In recent years, characteristic of extraction has been thoroughly investigated [7,8,9,10]. Global characteristic include depiction of the contours in the image, the style definition, texture characteristics and local characteristics [11,12]. Some example of global descriptors are from matrices and invariant moments as well as histogram dependent gradients [13]. Some problem relates to occlusion, viewing and lighting changes and local characteristics of imaging are being dealt with by global methods due to their insufficiency.

The extraction methods through native region that extract features from the local region of the image are well adapted to these issues. Such regions may be as small as easy or chosen by key points as image portions. Texture and color offers knowledge of significance information form the development of efficient features by confirming the strong recovery system output. The classic texture characteristic was derived from the grayscale images. The scale-invariant features transform (SIFT) is more productive, viable and precise descriptor in a cutting edge acknowledgement and characterization framework, among the diverse nearby local descriptor for grayscale images [14]. In order to capture the texture from color images, several variants are available. The SIFT color was evaluated and found to outperform a number of color descriptors. However, the SIFT color is an intensive computation, particularly when scaling the image or the

dimension of the database is increased. Ojala et al. [15], the LBP, often a significant descriptor of texture, has been found in several pattern recognition systems and in computer vision applications to be effective and strong. It preserves characteristics of local texture that are invariant for changes in lighting [16,17]. Most of the efforts have been put in texture recognition [18-21], face analysis [22-24], identification of facial expression [25-28], image recovery [29,30] and so forth, the LBP operator has been successfully used. Most research has been performed on the standard LBP operator and their gray-scale imaging models [31-34]. Color images on the internet are increasingly demanded and used for many realistic applications. Researchers have created descriptor images which denote color texture designs as well as LBP operators for gray scale images [35-39].

In this paper suggested operators MBPC and MBPH for color images which extracts color image structures that imitate the gray-scale texture extracted by the LBP operator. A vector of m components is called a color pixel and we create a hyperplane for that reason. The hyperplane is used as a threshold boundary with two classes of dividing color pixels. The value is assigned 1 if it is on a plane or above and 0 if it is below a plane, in a 3 × 3 neighborhoods of the current pixels. These operators proposed thus establishes spatial relationships between color pixels, which represent local texture characteristics. In a manner that matches LBP operator histogram for gray images, that may calculate binary pattern histograms extracted from color images. There are 256 histogram bins, while suggested operator's uses eight color pixels in the neighborhood, as features reflecting local image texture patterns. Proposed method is based on the channel color histogram (CH) from the H-specific (HIS) model, which is fusion with MBPC + MBPH. Among the best color image descriptors, most researcher frequently chosen the color histogram. Thus the MBPC+MBPH+CH solution proposes. Similarly, also suggested another solution MBPC + MBPH + FCH, where fuzzyfied color channel histogram [40] based on the H channel color histogram (CH) from the HSV color space is used. The purpose of this study to improve image retrieval rate of related images from each categories of different dataset efficiently.

Although the descriptor output is greatly interrelated in both settings, substantial discrepancies have to be taken into consideration while choosing the descriptors for large-scale jobs. For the best descriptors, a correlation review is given, indicating the best possible combination of its use.

This paper is categorized in the following way: In Section 2, given a color image description of those binary descriptors of the current state of art focused on the local trends. Section 3 derived the suggested MBPC and MBPH operator. In Section 4 one can consider the characteristics and the fusion of the MBPC and MBPH operator with the color histogram (CH) and fuzzyfied Color Histogram (FCH) respectively. Section 5 outlines the different dimension of similarity measurements and results used in applications of image retrieval. In Section 6 presented a comprehensive experimental analysis on different color image databases for their retrieval performance. In Section 7 the conclusion and future work are remarked finally.

II. A Taxonomy of Related Work

In this section, presents an outline of the firmly correlated works which have a place with the varieties of Local-Binary Patterns like strategies produced for the color images to use the benefit of the relationship between the color channels. An explained below, every method has its own advantages and disadvantages.

A. Local Binary Pattern (LBP)

Firstly proposed a method that describe local information very efficiently within an image [15]. The traditional LBP generates an 8-digit binary number that generates a binary pattern. For the convenience a binary pattern is transformed to be code usually a number in decimal. Within the grayscale image, a 3×3 block B_m has a central pixel C_m, compared to the surrounding pixels of C_m, the LBP coding will be done as follows:

$$LBP_{C_m} = \sum_{n=0}^{|B_m|-1} h(C_n - C_m)2^n \text{ h(t)} = \begin{cases} 1, t \geq 0. \\ 0, t < 0. \end{cases} \quad (1)$$

Where $|B_m|$ is the number of elements in B_m.

B. Uniform Local Binary Pattern (ULBP)

To reduce the feature vector scale, the uniform binary pattern is used in contrast with the LBP [15]. The LBP estimation of pixel (i, j) , let's represent in the $LBP_{p,redius}(i, j)$. In order to S mean the string of twofold qualities. Only those patterns of 2^p binary patterns (denoted as ULBP) which fulfil this requirements are referred to as Uniform:

$$\sum_{i=1}^{P} |S_i - S_{i-1}| + |S_0 - S_p| \leq 2 \quad (2)$$

where S_i denote the i^{th} bit of the string. The rest of the patterns are farmed regular and located into a single group. In all the uniform patterns is $P(P-1)+3$ that is less than 2P, especially if P is big. For P = 8 there are 256 and 59 patterns. Respectively in total LBP and ULBP pattern for example.

C. Multispectral Local Binary Pattern (MSLBP)

Mäenpää et al. [41] using RGB color channels and six adversary color pairs. Those opposing colors, which provide cross-linkage between values of colors and spatial relations, are used to obtain two color-structure characteristics. The three LBP-functional vectors can be accomplished by treating each channel of an RGB image like gray images [19], analogous to the LBP functionality of the gray scale. The following are derived from the six opposing LBP vectors:

$$\text{MSLBP}^{(i,j)}(x_c, y_c) = \sum_{p=0}^{p-1} S\left(v^i(x_p, y_p) - v^i(x_c, y_c)\right) \times 2^p \quad (3)$$

$where\ (i, j) = \{(1,2), (2,3), (3,1), (2,1), (3,2), (1,3)\}$, and

$$S\left(v^i(x_p, y_p) - v^i(x_c, y_c)\right) = \begin{cases} 1, if\ \left(v^i(x_p, y_p) - v^i(x_c, y_c)\right) \geq 0 \\ 0,\ otherwise \end{cases} \quad (4)$$

Here $v^i(x_c, y_c)$ is the center of pixel intensity of the image component j^{th} = 3 window, $v^i(x_p, y_p)$ is a neighborhood pixel intensity value of the image i^{th} color variable. There are 2304 MSLBP features, i.e. the function vector after nine LBP

operators have been concatenated. A high recognition tare is given by the method. Nevertheless, the vector size is too larger to decrease the recovery rate.

D. Local Color Vector Binary Pattern for Face Recognition (LCVBP)

In LCVBP method color angular patterns and color norm patterns are the two discriminative patterns [22].

$$f_{cn}^{p} = \varphi_{cn}\left(h_{cn}^{p}\right) \text{ and } f_{ca_{i,j}}^{p} = \varphi_{ca_{i,j}}\left(h_{ca_{i,j}}^{p}\right), for\ i < j) \quad (5)$$

$$i = 1, \ldots\ldots\ldots, K-1, and\ j = 2, \ldots\ldots\ldots, K.$$

Similar calculations may be performed for lower-sized features f_{cn}^{g} and $f_{ca_{i,j}}^{g}$ of h_{cn}^{g} and $h_{ca_{i,j}}^{g}$. The lower dimension features of the LBP histogram are joint at feature level by concentrating the lower dimension features in column order respectively in the following order for the proposed LCVBP feature of I^{p} and I^{g}.

$$f_{LCVBP}^{p} = [(f_{cn}^{p})\mathrm{T}\left(f_{ca_{1,2}}^{p}\right)\mathrm{T} \ldots \left(f_{ca_{1,K}}^{p}\right)\mathrm{T} \ldots \left(f_{ca_{K-1,K}}^{p}\right)\mathrm{T}]\mathrm{T} \quad (6)$$

$$f_{LCVBP}^{g} = [(f_{cn}^{g})\mathrm{T}\left(f_{ca_{1,2}}^{g}\right)\mathrm{T} \ldots \left(f_{ca_{1,K}}^{g}\right)\mathrm{T} \ldots \left(f_{ca_{K-1,K}}^{g}\right)\mathrm{T}]\mathrm{T} \quad (7)$$

E. Quaterninoic Local Ranking Binary Pattern (QLRBP)

This is another descriptor for color image. A QLRBP was developed by Lan et al. [42] to integrate multi-spectral channel color knowledge in color pictures, and a local quaternionic rating binary pattern was adopted. The operator QLRBP extracts the quaternionic representation (QR) of color image. Without having to treat every color channel individually, the QLRBP may manage all color channel directly within the quaternionic field. The ranking function can be expressed as:

$$R_{QLRBP}\left(\dot{q_m}, \dot{q_n}\right) = \delta_{CTQ(\dot{q_n}, \dot{p_1})} - \delta_{CTQ(\dot{q_m}, \dot{p_1})} \quad (8)$$

$$QLRBP_{\dot{q}_m} = \sum_{n=0}^{|S_m|-1} h\left(R_{QLRBP}\left(\dot{q_m}, \dot{q_n}\right)\right) 2^{n} \quad (9)$$

F. Multichannel Decoded Local Binary Pattern (MDLBP)

MDLBP based on decoder based local binary pattern $mdLBP_{t_2}^{n}(i,j)$ for pixel (i,j) from multichannel decoder map [43] $mdM^{n}(i,j)$ and t_2 can be computed as:

$$mdLBP_{t_2}^{n}(i,j) = \begin{cases} 1, if\ mdM^{n}(i,j) = (t_2 - 1) \\ 0, otherwise \end{cases} \quad (10)$$

For $\forall t_2 \in [1, 2^{c}]$ and $\forall n \in [1, N]$.

G. Color Histogram Creation Method based on Fuzzyfication (FCH)

A motivation behind picking up the HSV color space is that it is recognizably uniform and approximates how individuals perceives. The primary expiation, however, is that HSV color space has been discovered to be stronger than other color spaces in various retrieval experiments. The fuzzy link based approach is used to construct a histogram in the descriptor. More than one histogram output is specified by the term "fuzzy-linking" [40]. The input channels are described in the following fuzzy sets:

- The channel Hue(H) is divided into 10 fuzzy regions,
- The channel Saturation (S) is divided into 3 fuzzy regions,
- The channel Value (V) is divided into 3 fuzzy regions.

$$\mu_A(x) = \begin{cases} 0, (\mathrm{X} < t) \text{or } (\mathrm{X} > \mathrm{v}) \\ \frac{\mathrm{X}-\mathrm{t}}{\mathrm{u}-\mathrm{t}}, \mathrm{t} \le \mathrm{X} \le \mathrm{u} \\ 1, \mathrm{u} \le \mathrm{X} \le \mathrm{w} \\ \frac{\mathrm{v}-\mathrm{X}}{\mathrm{v}-\mathrm{w}}, \mathrm{w} \le \mathrm{X} \le \mathrm{v} \end{cases} \quad (11)$$

Where t is the lower limit, v is upper limit, u is lower support limit and w is upper support limit, also t < u < w < v. The membership features are displayed in Fig. 1 to 3. For the H channel, the final fuzzy histogram includes only 10 bins out of the 12 bins. The prevailing hues in each image can promptly be taken note. As portrayed in the accompanying area, the histogram in the proposed framework has demonstrated to be an instrument for accurate image recovery.

Histogram bins that are shown in Fig. 1 to 3 is concerning: (1) Red, (2) Orange, (3) Yellow, (4) Light Green, (5) Green, (6) Spring Green, (7) Cyan, (8) Azure, (9) Blue, (10) Violet, (11) Magenta and (12) Rose Red for H Channel. Correspondingly, for S channel receptacles are: (1) Low, (2) Medium and (3) High Saturation. What's more, for V Channel receptacles are: (1) Dark, (2) Light and (3) Bright.

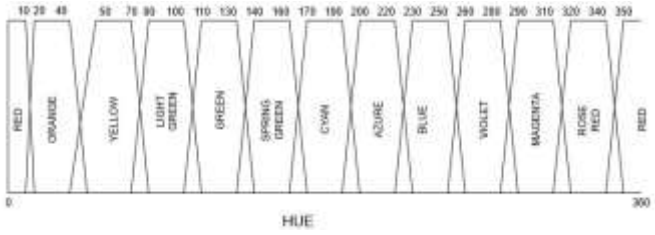

Fig. 1. Membership Function of Hue Color.

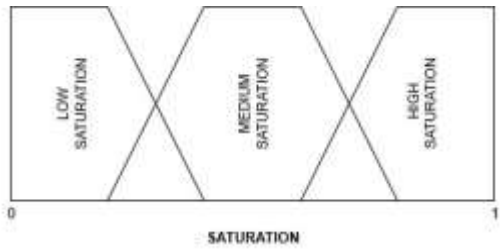

Fig. 2. Membership Function of Saturation Channel.

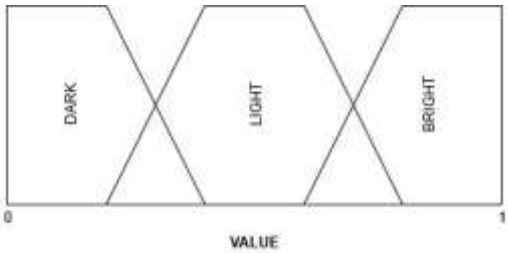

Fig. 3. Membership Function of Value Channel.

III. Proposed Work

The Median Binary Pattern for color (MBPC) is first briefly described in this section.

A. Median Binary Pattern (MPB)

For gray scale images, the classic MBP [50] operator is described. For a circular symmetric neighbor group of P members, the common form of the operator is represent as: $R(x_p, y_{p)}$ and median (x_m, y_m), as defined by $MBP_{p,r}$, R(x_m, y_m):

$$\mathrm{MBP}_{\mathrm{P,R}}\,(X_m, Y_m) = \sum_{p=0}^{p-1} S\left(I(x_p, y_p) - I(x_m, y_m)\right) \times 2^p \qquad (12)$$

Where P is the quantity of neighbors and has the estimation of solidarity. The operator of the MBP is invariant with repetitive gray scale changes as the edge doesn't rely upon the intensity. The example examined is the result of spatial associations in the specific area. On the off chance that a specific neighborhood has no correlation, it is known as a spot.

Where

$$S\big(\mathrm{I}(\mathrm{x_p}, \mathrm{y_p}) - \mathrm{I}(\mathrm{x_m}, \mathrm{y_m})\big) = f(\mathrm{x}) = \begin{cases} 1, \text{ if } \mathrm{I}(\mathrm{x_p}, \mathrm{y_p}) - \mathrm{I}(\mathrm{x_m}, \mathrm{y_m}) \geq 0 \\ 0, otherwise, \end{cases} \qquad (13)$$

and I(x_p, y_p) is a pixel location intensity (x_p, y_p). 8 neighborhood pixels at (x, y) are called in their simplest form, i.e. $P = 8$, and $R = 1$. Here, the MBP operator divides the image into two classes of pixels based on the median value of the configuration. Note that MBP compares two levels of severity, which influence the structure locally as well. Such patterns constitute the fundamental element of proposed texture description. The MBP operator produces binary patterns called MBP patterns, which range from 0 to 2^P-1. For each pixel of an image, MBP patterns are obtained under histograms with MBP patterns. These histograms define the texture of an image with a gray scale. When the value of P is higher, than scale of histogram patterns will be greater.

In MBP the threshold directly does not depend on amount of pixel intensity therefore it is invariant to monotonic gray scale changes in the image. Through the spatial interfaces in the given locality as a result the pattern information has been detected. Fig. 4 shows the calculation of MBP.

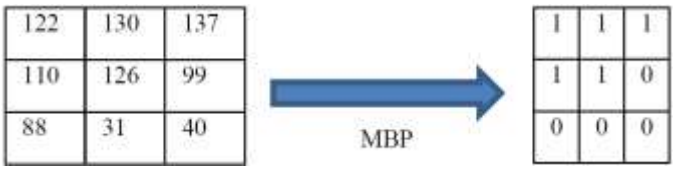

Fig. 4. Showing MBP, the Median Value is 110.

B. The Suggested MBPC Operator

The suggested MBPC operator uses a hyperplane in the m dimensions for partitioning or thresholding of color pixels. As m= 3 in this case, 3D space is hyper-plan. Namely a hyper-ellipsoid or a hyper-cube, a hyper-sphere, are other threshold alternatives, they are, however, not as effective as a hyperplane. After extensive experiments with these threshold alternatives, this work came to this conclusion. The future challenge is to construct a thresholding in 3D color that is performed as follows. The color pixel elements of RGB color space is to represented by the vector $\boldsymbol{I}(x, y) = (r(x, y), g(x, y), b(x, y)$ or, simply, $\boldsymbol{I} = (r, g, b)$. Consequently, the color variable of m is 3. The local window $(2R + 1) \times (2R + 1)$ of size is defined as the corresponding color vector(r_m, g_m, b_m), $R \geq 1$, median at pixel m. Let I_p = (r_p, g_p, b_p) be a pixel p of the neighborhood. Within the color space, the color plane L is established. Through specifying the normal and a reference point in the color space a plane is derived. The level is inferred by characterizing the typical to the plane and a reference point in the color space. Let $n = (n_1, n_2, n_3)$ be denoted as normal to the plane and R_o= (r_o, g_o, b_o) be the reference point,

At the point the condition of the level with the normal vector n and the reference point R_o is presented as:

$$n.(I_p - R_o) = 0. \qquad (14)$$

or,

$$n1(r - r_0) + n2(g - g0) + n3(b - b0) = 0. \qquad (15)$$

The consequence of the dot product between the vector n and the vector generated by joining in two classes R_o = (r_o, g_o, b) to $Ip = (r, g, b)$ space. The vector $I_p - R_o$ produces every pixel on or above the plane. The color plane separates the color into unique class and all the other pixels below the plane into another class. There are many ways to choose normal vector n but a line that joins the dark pixel $(0, 0, 0)$ and the pure white pixel $(1, 1, 1)$ is an evident choice. It reflects the gray line and all primary colors R, G and B are equally present. The median pixel I = (r_m, g_m, b_m) of the square neighborhood would be an obvious choice for the reference point. Color plane is defined, which is normal for line connections $(0, 0, 0)$ and $(1, 1, 1)$, with these values of the two parameter, and passes over R_o= I_m= (r_m, g_m, b_m). It enables neighborhood pixel thresholding method $I_p, p = 0, 1, \dots, P - 1$ into two classes: those above or on the plane, and some below the plane. Here, P reflects the total number of neighborhood pixels. The following expression can be assessed for a decision to this effect.

$$E_v(I_p) = E_v(r, g, b) = n_1(r_p - r_c) + n_2(g_p - g_c) + n_3(b_p - b_c), \qquad (16)$$

The color pixel $I_p = (r_p, g_p, b_p,)$ is above or above the plane if $E(I_p) \geq 0$ and below the plane if $E(I_P) < 0$. Therefore the color pixels are divided into two groups with a clearly defined process in the median pixel neighborhood. An extension of binary patterns on local grayscale, which is obtained by restricting gray values to the gray value for a median pixel (x_m, y_m) of the local window can be considered.

C. The Suggested MBPH Operator

MBP is a classical gray scale operator that cannot be further drawn-out to color images since a color pixel represented a vector quantity of R, G, and B components and a scalar quantity was the gray scale pixel. Consequently, for

color pixels to get a binary set, a comparison of the Eq. (18) type cannot be made.

The proposed Median binary patterns of the hue (H) component (MBPH) from HSI model.

$$MBPH_{P,R}(x_m^h, y_m^h) = \sum_{p=0}^{p-1} S\left(I(x_p^h, y_p^h) - I(x_m^h, y_m^h)\right) \times 2^p \quad (17)$$

Where

$$S\left(I(x_p^h, y_p^h) - I(x_m^h, y_m^h)\right) = \begin{cases} 1, if\ I(x_p^h, y_p^h) - I(x_m^h, y_m^h) \geq 0 \\ 0, otherwise \end{cases} \quad (18)$$

$I(x_p^h, y_p^h)$, is an intensity of pixel at (x,y), the color component in H plane of HSI color image model and (x_m^h, y_m^h) is a median value of selected patch if an image.

IV. Fuzzy Color Histogram (FCH) and Median Binary Pattern of the HUE Component (MBPH) and their Fusion with MBPC Features

Most of the time color features are dominant to identify objects as a whole from the image. The color texture may be obtained from colored image that represents in Hue (H) component of the HIS model. Therefore, the hue element is a normal option for segmenting an image dependent on color. To fuse with different features, suggested method uses fuzzy color histogram (FCH), MBPC of a color image driven by RGB color color space, and MBP is driven by the hue component of HSI image, which is then called MBPH. By using the following color conversion function from a colour image inside the color space of the RGB, the component hue is achieved.

$$H(i,j) = \begin{cases} \theta(i,j)\ , if\ b(i,j) \leq g(i,j) \\ 2\pi - \theta\ if\ b(i,j) > g(i,j) \end{cases} \quad (19)$$

Where

$$\theta(i,j) = \cos^{-1}\left\{ \frac{\frac{1}{2}[(r(i,j)-g(i,j))+(r(i,j)-b(i,j))]}{\left[(r(i,j)-g(i,j))^2+(r(i,j)-b(i,j))(g(i,j)-b(i,j))\right]^{1/2}} \right\} \quad (20)$$

A gray scale image is treated as $H(x,y)$ whose median binary patterns are in a manner identical to the median gray scale image binary patterns. Such features are called MBPH features. The features of MBPH is computed as follows.

The median of a window $(2R+1)*(2R+1)$ be (x_m, y_m). The features of MBPH are found as

$$MBPH(x_m, y_m) = \sum_{p=0}^{P-1} F_m(Q_p) * 2^P \quad (21)$$

Where

$$F_m(Q_p) = \begin{cases} 1\ if\ H(x_p, y_p) \geq H(x_m, y_m) \\ 0\ otherwise. \end{cases} \quad (22)$$

Here (x_p, y_p) is the coordinates of a neighborhood pixel.

Sometimes color histogram image descriptors especially useful. Fuzzy color histogram (FCH) is an extended version of CH descriptor.

Through separating them through image scale before their fusion, all histogram bins are normalized. The MBPC, MBPH and FCH are three feature vectors, of size s_c, s_h and s correspondingly, are combined to create a single dimension vector of size $s_c + s_h + s$ whose components are represented by.

$$\{MBPC[0], MBPC[1], \ldots., MBPC[s_c - 1], MBPH[0], MBPH[1], \ldots., MBPH[s_h - 1], FCH[0], FCH[1], \ldots., FCH[s-1]\}. \quad (23)$$

V. Similarity Measures and Estimation Metrics

A. Similarity Measures

Various similarity measures have been suggested in the literature for image processing systems. Retrieval in the CBIR system, performance of retrieval not only depends on robust features but also measures through different similarity functions available in the literature. When work with histogram-based feature vectors, this dimension will underpin option of similarity tests. Four of these common parallels are Euclidean distance, chi-square, extended-Canberra and square-chord for histogram dependent function vectors. Certain distance measurements widely employed, including histogram cross section, $L1$-norm, $L2$-norm, Jeffrey gap, cos-correlation, etc., are not as successful as the previous ones [53]. With respect to such a similarity metric, evaluate the performance comparison and try to find an effective distance measure which provides the finest total recovery outcomes. It provides the following descriptions of the distance measures.

Let $FV_i^q\ and\ FV_i^{db}$ represents the i[th] feature components of image query 'q' and image database 'db', respectively. Feature vector size indicate by FVSize. Following is the formula of distance measures:

Euclidean Distance

$$\text{Distance}_{Euclidean} = \sqrt{\sum_{i=0}^{n}(|Q_i - D_i|)^2} \quad (24)$$

Extended-Canberra Distance:

$$Distance_{Extended-Canbera}(q, db) = \sum_{i=0}^{FVSize-1} \frac{\left|FV_i^q - FV_i^{db}\right|}{(FV_i^q + \mu^q) + (FV_i^{db} + \mu^{db})} \quad (25)$$

Chi-square

$$Distance_{Chi}(q, db) = \sum_{i=0}^{FVSize-1} \frac{(FV_i^q - FV_i^{db})^2}{FV_i^q + FV_i^{db}} \quad (26)$$

Square – Chord distance

$$Distance_{Square-Chord}(q, db) = \sum_{i=0}^{Size-1} (\sqrt{FV_i^q} - \sqrt{FV_i^{db}})^2 \quad (27)$$

B. Estimation Metrics

All images in the experiments is used as a query image in the database. P(N) and R(N) precision can be used to measure the performance of the image retrieval. Top N images described in [54].

$$P(N) = \frac{I_o}{N};\ R(N) = \frac{I_o}{M} \quad (28)$$

Where M is the total number of images that are identical to query images in the dataset and I_o is the total number of relevant images from higher index positions? The sum of all P(n) exact values is the average precision of the single query $\bar{P}(q), n = 1,2, \dots, N, i.e.$

$$\bar{P}(q) = \frac{1}{N} \sum_{n=1}^{N} P(n). \quad (29)$$

For each queries Q, the mean average precision (mAP) is the mean of the average scores:

$$mAP = \frac{1}{Q} \sum_{q=1}^{Q} \bar{P}(q). \quad (30)$$

If the number of the related images in each class differ, the graph P − R is not a satisfactory indicator. The *mAP* measure in [55].

VI. Results and Discussions

This section presents multiple experimental results which demonstrate the effectiveness and comparison [52] of the suggested methods with those of the closely linked operators of color textures, such as local bilateral component image patterns, LCVBP, MSLBP, MDLBP and QLRBP. For MDLBP operators, the decoder operator performs better than the adder operator. Therefore, decoder operator is considered for the performance comparison. The LBP image components are essentially an extension of the LBP to the R, G and B components of the color image. Another effective global descriptor for texture feature extraction is a Gabor filter which has been applied to gray scale images for texture image retrieval [44-49].

A. Datasets

To analyzing the proposed method three datasets namely Wang, Corel-5K and Corel-10K are used. In the following, these datasets is briefly explained [51].

Wang [53]: It comprises 1000 color images separated into 10 groups of 100 images each. It includes one of Corel's image databases. Every class includes 265 x 384 or 384 x 256 pixel resolution images. The 10 classes of Wang image database are: African tribe people, Bus, Dinosaur, Flower, Beach, Elephant, Buildings, Food, Horse and Glacier.

Corel- 5K [55]: This dataset contains 50 groups of images and each group has image of size 128 × 192 or 192 × 128 pixels in JPEG format. Each group has 100 images, with different substance like mountain, tiger, fort, mushroom, car, ticket, ocean etc. in total 5000 images.

Corel- 10K [55]: This dataset contains 100 groups of images and each group has image of size 128 × 192 or 192 × 128 pixels in JPEG format. Each category has 100 images of various substances like rose, sunset, cat, train, duck, fish, judo-karate, etc. in total 10,000 images.

B. Comparison with Existing Methods

In contrast with the following techniques, the findings of the suggested methods are compared: mean average precision (mAP) performance is based on LBP, ULBP, MSLBP, LCVBP, QLRBP, and MDLBP. The results also list the number of features used by all techniques. The methods proposed are also applied separately by fusion of their characteristics in two combinations. MBPH, FCH are separate processes, while MBP+MBPH+CH while MBP+MBPH+FCH are two variations. Such strategies are tested to determine their relative efficiencies and to define the best solutions for high precision and low recovery times. The benefit of speed is therefore that the feature vector with low dimensional dimensions does not cause a great deal of recovery precision. There is a similar trend with MBPH and FCH operators, which is described in the following experimental analysis. The results are comparable with the following approaches: LBP, ULBP, LCVBP, MSLBP, QLRBP, GABOR, MDLBP, MBPC+MBPH+CH, and MBPC+MBPH+FCH.

Proposed method is compared the following approaches. In order to evaluate output of a value of N, a deeper examination of the amount of the images obtained was conducted, and the results for N=1 to 12 were given from 100 values of N, in Table I.

Table II shows the mAP values, attained by the several method includes top 100 image ($N = 100$) of the Wang dataset. The images in all databases are used as images for queries. It is noted from the table that, with the square chord distance, the MBPC+MBPH+FCH solution proposes the highest mAP of 63.9. The efficiency of the resulting method is significantly improved when FCH features fuse with MBPC+MBPH to obtain the MBPC+MBPH+FCH method. Finally, the efficiency of the estimated square chord interval is better seen in the mAP values displayed in Table II. The values of precision versus recall are shown in Fig. 5 for 9 methods (7 existing, 2 proposed) that produce the overall results.

Euclidean, Chi-sqaure, Extended Canberra and Square-Chord obtained average mAP value are 57.32%, 52.23%, 58.08%, and 63.9%, respectively.

The results shown by Table III is based on Corel-5K dataset. The proposed MBPC + MBPH + FCH method achieves a maximum mAP value of 42.47% followed by the MBPC + MBPH + CH method that results in a mAP of 41.88%. MDLBP, which uses Square-Chord, reaches the next largest mAP value. GABOR, which is 37.12 %, is the fourth largest mAP. The decreased mAP values of other existing methods performance is: LCVBP (36.4%), LBP (35.41), MSLBP (35.33), QLRBP (35.22), and ULBP (32.88%). The difference of mAP values from the proposed MBPC + MBPH + CH and MBPC + MBPH + FCH, which is insignificant, is only 0.59, whereas the size of feature vector differences in the proposed method is significant. The distance measured by Euclidean, Chi-sqaure, Extended Canberra and Square-Chord obtained average mAP value are 36.35%, 31.05%, 37.9%, and 42.47%, respectively for method MBPC + MBPH + FCH. Fig. 6 plots the precision and recall values of existing and suggested approaches. The suggested methods are seen to outperform the conventional methods for all recall values.

The findings for Corel-10 K are shown in Table IV. The development for mAP values is closed to the development for datasets Wang and Corel-5k. The suggested MBPC + MBPH + FCH solution reaches the 33.89% highest value of mAP. It should be noted here that although the mAPs of these two

proposed methods vary slight difference by 1 percent. Although the second largest value is obtained by MDLBP, which is 33.23% with 2048 features size is higher than compared with the proposed methods. Therefore, the third largest value of mAP, is attained by MBPC+MBPH+CH that is 32.89% by using 1055 features. Precision versus recall values for N=100 is shown in Fig. 7.

TABLE I. NUMBER OF SIMILAR IMAGES (IN PERCENT) OBTAINED FOR EACH CATEGORIES FROM WANG DATASET VALUE OF $N(N = 1\ to\ 12)$ BY THE SUGGESTED MBPC+MBPH+CH (METHOD X) AND BY MBPC+MBPH+FCH (METHOD Y)

N	**Class**																			
	African		**Beach**		**Building**		**Bus**		**Dinosaur**		**Elephant**		**Flower**		**Horse**		**Glacier**		**Food**	
	X	*Y*	*X*	*Y*	*X*	*Y*	*X*	*Y*	*X*	*Y*	*X*	*Y*	*X*	*Y*	*X*	*Y*	*X*	*Y*	*X*	*Y*
1	100	100	100	100	100	100	100	100	100	100	100	100	100	100	100	100	100	100	100	100
2	94	92	85	80	86	89	96	99	100	100	92	91	97	99	97	99	76	77	90	92
3	91	87	76	70	77	84	93	98	99	99	85	85	95	97	96	98	68	68	85	87
4	88	84	73	66	73	80	93	96	99	99	82	79	95	97	94	98	63	63	83	84
5	86	83	69	61	68	78	93	96	99	99	77	75	94	96	91	97	59	60	80	83
6	85	82	67	59	66	75	92	96	99	99	76	72	93	96	90	96	57	57	79	80
7	83	82	66	57	63	73	91	95	99	99	73	68	93	96	87	96	55	55	78	79
8	82	81	64	55	60	72	90	94	99	99	72	66	93	96	86	96	54	54	76	76
9	81	80	63	54	58	69	89	94	99	99	69	63	92	95	85	95	52	52	74	75
10	80	79	62	53	58	68	88	94	99	99	68	61	92	95	84	94	50	50	72	74
11	79	79	61	52	56	68	87	93	99	99	68	58	91	94	83	94	48	48	70	72
12	78	78	60	51	55	66	87	93	99	99	66	57	91	94	82	94	47	47	68	71

TABLE II. MEAN AVERAGE PRECISION (MAP) IN PERCENT FOR N = 100 OBTAINED USING VARIOUS APPROACHES ON WANG DATASET

	Method	No. of features	Euclidean	Chi-square	Extended-Canberra	Square chord
Existing	LBP [15]	3 × 256 = 768	45.94	55.28	56.93	55.33
	ULBP[15]	3 × 59 = 177	48.11	53.34	54.19	53.37
	MSLBP[41]	9 × 256 = 2304	50.20	59.86	60.62	59.86
	LCVBP[22]	4 × 59 = 236	47.21	53.52	56.83	53.44
	QLRBP[42]	3 × 256 = 768	45.18	53.47	56.03	53.50
	GABOR[54]	96	49.10	58.86	59.53	58.91
	MDLBP[43]	8 × 256 = 2048	50.10	59.58	60.82	59.58
Proposed	MBPC_MBPH_CH	=1055	53.67	50.77	57.93	60.01
	MBPC_MBPH_FCH	=1631	57.32	52.23	58.08	63.90

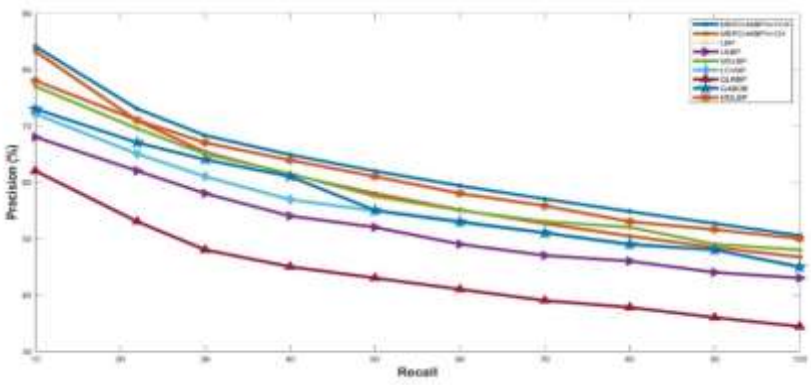

Fig. 5. Precision-Recall Curve for Existing and Proposed Methods (MBPC + MBPH + FCH and MBPC + MBPH + CH) for N = 100 on Wang Dataset.

TABLE III. MEAN AVERAGE PRECISION (MAP) IN PERCENT FOR N = 100 OBTAINED USING VARIOUS APPROACHES ON COREL-5K DATASET

	Method	No. of features	Euclidean	Chi-square	Extended-Canberra	Square chord
Existing	LBP [15]	3 × 256 = 768	27.43	35.38	35.75	35.41
	ULBP[15]	3 × 59 = 177	27.21	32.87	34.26	32.88
	MSLBP[41]	9 × 256 = 2304	28.1	35.53	39.95	35.33
	LCVBP[22]	4 × 59 = 236	29.5	36.39	37.95	36.4
	QLRBP[42]	3 × 256 = 768	28.12	35.31	36.54	35.22
	GABOR[54]	96	29.48	37.18	36.95	37.12
	MDLBP[43]	8 × 256 = 2048	29.56	37.89	39.99	38.08
Proposed	MBPC_MBPH_CH	=1055	36.31	32.59	38.52	41.88
	MBPC_MBPH_FCH	=1631	36.35	31.05	37.9	42.47

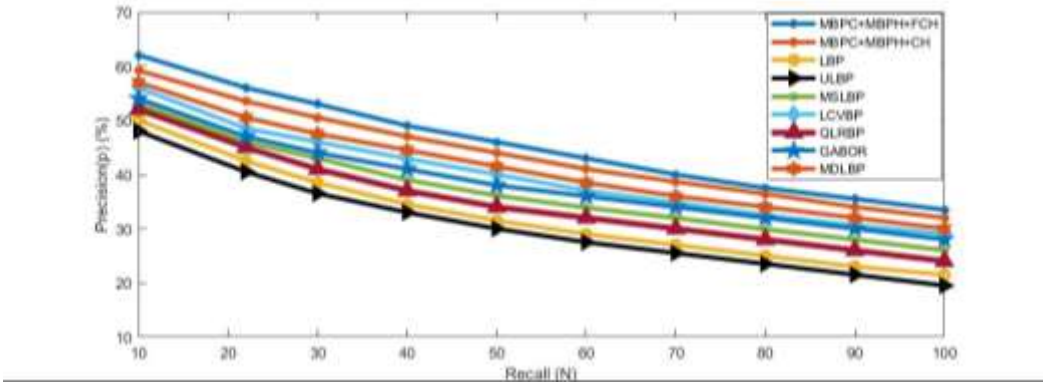

Fig. 6. Precision-Recall Curve for Existing and Proposed methods (MBPC + MBPH + FCH and MBPC + MBPH + CH) for $N = 100$ on Corel-5K Dataset.

TABLE IV. MEAN AVERAGE PRECISION (MAP) IS PRESENT FOR N = 100 OBTAINED USING VARIOUS APPROACHES ON COREL-10 K DATASET

	Method	No. of features	Chi-square	Extended-Canberra	Square chord
Existing	LBP [15]	3 × 256 = 768	28.97	29.33	28.98
	ULBP[15]	3 × 59 = 177	26.96	28.08	26.97
	MSLBP[41]	9 × 256 = 2304	28.99	31.69	28.86
	LCVBP[22]	4 × 59 = 236	29.25	29.72	29.26
	QLRBP[42]	3 × 256 = 768	26.4	27.64	26.39
	GABOR[54]	96	28.06	29.68	28.06
	MDLBP[43]	8 × 256 = 2048	31.83	33.97	33.23
Proposed	MBPC_MBPH_CH	=1055	25.16	31.19	32.89
	MBPC_MBPH_FCH	=1631	23.89	31.30	33.89

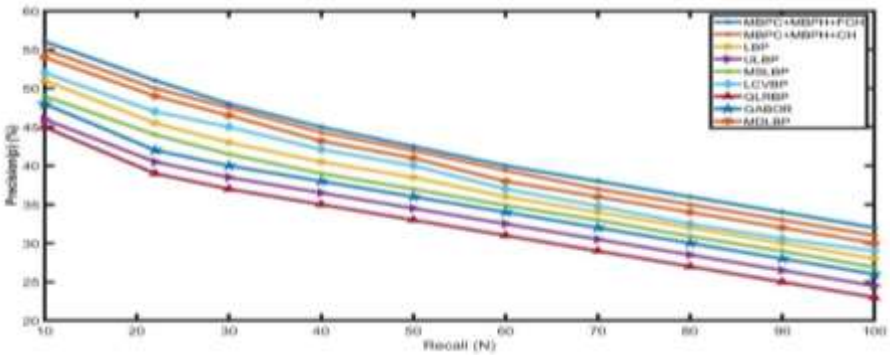

Fig. 7. Precision-Recall Curve for Existing and Proposed Methods (MBPC + MBPH + FCH and MBPC + MBPH + CH) for $N = 100$ on Corel-10K Dataset.

VII. Conclusion and Future Work

In the Color Image Retrieval issue the suggested median binary patterns (MBPC) for color textures are relatively efficient. The precision of recovery is further improved by the derivation of local binary patterns of the HSI color space (H) variable, known as the MBPH. An effective color image descriptor is the Color Histogram (CH) and is used for improving recovery performance using the proposed methods. If such color descriptors have been combined, the output has been evaluated individually as well as in their mixture types. Since both methods are focused on standardized histograms it is a concatenation method that incorporates such functions. There are also strong variations in LBPC and LBPH. Exhaustive performance experimental analysis shows, compared with the significant available local texture based on color, the descriptor and multichannel decoded local binary pattern (MDLBP) of the suggested MBPC+MBPH+FCH method reaches the most elevated estimation of mAP over all datasets. Compared to the strongest current MDLBP system with a large function aspect (2048), it offers far more effective outcomes of recovery at low device costs. The experimental findings also demonstrate that Square chord distance calculation outperforms all the significant distance measurements to award certain approaches the maximum mAP values in all datasets. In future, other effective methods may also be combined to get efficient image retrieval. Feature selection method may also use to obtain a prominent feature subset to improve the retrieval performance.

References

[1] Furht, B. “Encyclopedia of multimedia (2nd ed.). Springer Science & Business Media”, 2008.

[2] Lin, C.-H. , Chen, H.-Y. , & Wu, Y.-S. “Study of image retrieval and classification based on adaptive features using genetic algorithm feature”, Expert Systems with Applications, Vol 41 (15), pp. 6611–6621, 2014.

[3] Hiwale,S. S. & Dhotre, D. “Content-based image retrieval: Concept and current practices”, Paper presented at the Electrical, Electronics, Signals, Communication and Optimization (EESCO), 2015 international conference on, Visakhapatnam, India. 2015.

[4] M. Swain , D. Ballard , Color indexing, Int. J. Comput. Vis. Vol.7 (1), pp. 11–32, 2017.

[5] Ot´avio A.B. Penatti, Eduardo Valle, Ricardo da S. Torres, Comparative study of global color and texture descriptors for web image retrieval, Journal of Visual Communication and Image Representation, Vol. 23, Issue 2, pp. 359-380, ISSN 1047-3203, 2012.

[6] L. Liu, S. Lao, P. W. Fieguth, Y. Guo, X. Wang and M. Pietikäinen, "Median Robust Extended Local Binary Pattern for Texture Classification," in IEEE Transactions on Image Processing, Vol. 25, no. 3, pp. 1368-138, 2016.

[7] C. Zhu , C.-H. Bichot , L. Chen , Image region description using orthogonal combination of local binary patterns enhanced with color information, Pattern Recognit. Vol. 46, pp. 1949–1963, 2013.

[8] J. Li, N. Sang, C. Gao , Completed local similarity pattern for color image recognition, Neurocomputing Vol. 182, pp. 111–117, 2016.

[9] Y. Zhao, D. Huang, W. Jia, Completed local binary count for rotation invariant texture classification, IEEE Trans. Image Process. Vol. 21 (10), pp. 492–4497, 2012.

[10] S. Liao, M. Law, A. Chung, Dominant local binary patterns for texture classification, IEEE Trans. Image Process. Vol. 18 (5), pp. 1107–1118, 2009.

[11] M. Heikkilä, M. Pietikäinen, C. Schmid, Description of interest regions with local binary patterns, Pattern Recognition. Vol. 42 (3), pp. 425–436, 2009.

[12] L. Nanni, A. Lumini, S. Brahnam, Local binary patterns variants as texture descriptors for medical image analysis, Artif. Intell. Med. Vol. 49 (2), pp.117–125, 2010.

[13] N. Dalal, B. Triggs , Histograms of oriented gradients for human detection, in: Proceedings of the IEEE Conference on Computer Vision and Pattern Recogni- tion (CVPR), pp. 886–893, 2005.

[14] D.G. Lowe, Distinctive image features from scale-invariant keypoints, Int. J. Comput. Vis. Vol. 60 (2),91–110, 2004.

[15] Ojala T., M. Pietikäinen, T. Maenpää, Multiresolution gray-scale and rotation invariant texture classification with local binary patterns, IEEE Trans. Pattern Anal. Mach. Intell. Vol. 24 (7), pp. 971–987, 2002.

[16] R.M. Haralick, K. Shangmugam, Textural feature for image classification, IEEE Trans. Syst. Man Cybern. Vol. 6, pp. 610–621 SMC-3, 1973.

[17] H. Tamura, S. Mori, T. Yamawaki, Texture features corresponding to visual per- ception, IEEE Trans. Syst. Man Cybern. Vol. 8 (6) pp. 460–473, 1978.

[18] T. Mäenpää, M. Pietikäinen , T. Ojala , Texture classification by multi-predicate local binary pattern operators, in: Proceedings of the International Conference on Pattern Recognition (ICPR), pp. 3951–3954, 2000.

[19] T. Mäenpää, T. Ojala, M. Pietikäinen , M. Soriano , Robust texture classification by subsets of local binary patterns, in: Proceedings of the International Conference on Pattern Recognition (ICPR), pp. 3947–3950, 2000.

[20] M. Pietikäinen,T. Mäenpää,V. Jaakko , Color texture classification with color histograms and local binary patterns, in: Workshop on Texture Analysis in Machine Vision, pp. 109–112, 2002.

[21] Y. Guo, Z. Guoying , M. PietikäInen , Discriminative features for texture description, Pattern Recognit. Vol. 45 (10), pp. 3834–3843, 2012.

[22] S.H. Lee, J.Y. Choi, Y.M. Ro, K.N. Plataniotis , Local color vector binary patterns from multichannel face images for face recognition, IEEE Trans. Image Process. Vol. 21 (4), pp. 2347–2353, 2012.

[23] T. Ahonen, A. Hadid , M. Pietikäinen , in: Face Recognition With Local Binary Patterns Lecture Notes in Computer Science, 3021, Springer-Verlag, Berlin Heidelberg New York, pp. 469–481, 2004.

[24] T. Ahonen, A. Hadid, M. Pietikäinen, Face description with local binary patterns: application to face recognition, IEEE Trans. Pattern Anal. Mach. Intell. Vol. 28 (12),pp. 2037–2041, 2006.

[25] C. Shan, S. Gong, P.W. McOwan, Robust facial expression recognition using local binary patterns, in: Proceedings of IEEE International Conference of Image Processing,Vol. 2, pp. 370–373, 2005.

[26] Z. Guoying, M. Pietikainen, Dynamic texture recognition using local binary pat- terns with an application to facial expressions, IEEE Trans. Pattern Anal. Mach. Intell. Vol. 29 (6), pp.915–928, 2007.

[27] C. Shan, S. Gong, P.W. McOwan, Facial expression recognition based on local binary patterns: a comprehensive study, Image Vis. Comput. Vol. 27 (6), pp. 803–816, 2009.

[28] S. Zhang , X. Zhao , B. Lei , “Facial expression recognition based on local binary patterns and local fisher discriminant analysis”, WSEAS Trans. Sig. Process. Vol. 8 (1), pp. 21–31, 2012.

[29] V. Takala, T. Ahonen, M. Pietikäinen, Block-based methods for image retrieval using local binary patterns, in: Proceedings of Scandinavian Conference on Image Analysis, pp. 882–891, 2005.

[30] O.A.B. Penatti, E. Valle, R.S. Torres, Comparative study of global color and tex- ture descriptors for web image retrieval, J. Vis. Commun. Image Represent. Vol. 23 (2), pp. 359–380, 2012.

[31] Satpathy, X. Jiang, H. Eng, Lbp based edge texture features for object recognition, IEEE Trans. Image Process. Vol. 23 (5), pp. 1953–1964, 2014.

[32] Fernández, M. Álvarez, F. Bianconi, Texture description through histograms of equivalent patterns, J. Math. Imaging Vis. Vol. 45 (1), pp. 76–102, 2013.

[33] L. Nanni, A. Lumini, S. Brahnam, Survey on lbp based texture descriptors for image classification, Expert Syst. Appl. Vol. 39 (3), pp. 3634–3641, 2012.

[34] Nguyen, P. Ogunbona, W. Li, A novel shape-based non-redundant local binary pattern descriptor for object detection, Pattern Recognit. Vol. 46 (5), pp. 1485–1500, 2013.

[35] S. Manjunath, J.-Ohm, V. V. Vasudevan and A. Yamada, "Color and texture descriptors," in IEEE Transactions on Circuits and Systems for Video Technology, Vol. 11, no. 6, pp. 703-715, June 2001.

[36] D. Huang, S. Caifeng , A. Mohsen , W. Yunhong , C. Liming , Local binary patterns and its application to facial image analysis: a survey, IEEE Trans. Syst. Man Cybern. Part C Vol. 41 (6), pp. 765–781, 2011.

[37] Liu, G. H., Yang, J. Y., & Li, Z. Content-based image retrieval using computational visual attention model. Pattern Recognition, Vol. 48(8), pp. 2554–2566, 2015.

[38] Shakoor, M. H., & Boostani, R. Radial mean local binary pattern for noisy texture classification. Multimedia Tools and Applications, Vol. 77(16), pp. 21481–21508, 2018.

[39] M. Sotoodeh, M.R. Moosavi and R. Boostani, A novel adaptive LBP-based descriptor for color image retrieval, Expert Systems With Applications, Vol. 127, pp. 342–352, 2019.

[40] Johari P.K., Gupta R.K., Retrieval of Content-Based Images by Fuzzified HSV and Local Textural Pattern. In: Intelligent Computing Applications for Sustainable Real-World Systems. ICSISCET 2019. Proceedings in Adaptation, Learning and Optimization, Vol. 13, pp. 219-229 Springer, Cham.

[41] T. Mäenpää,M. Pietikäinen,J. Viertola, Separating color and pattern information for color texture discrimination, in: Proceedings of 16th International Conference on Pattern Recognition, Vol.1, pp. 668–671, 2002.

[42] Rushi Lan, Yicong Zhou, and Yuan Yan Tang, Quaternionic Local Ranking Binary Pattern: A Local Descriptor of Color Images, IEEE transactions on image processing, Vol. 25, no. 2, pp. 566-579, 2015.

[43] S.R. Dubey, S.K. Singh, R.K. Singh, Multichannel decoded local binary patterns for content-based image retrieval, IEEE Trans. Image Process. Vol. 25 (9), pp. 4018–4032, 2016.

[44] G.J. Burghouts, J.-M. Geusebroek, Performance evaluation of local color invariants, Comput. Vis. Image Understand. Vol. 113 (1) pp. 48–62, 2009.

[45] A. Yamada, "Color and texture descriptors," in IEEE Transactions on Circuits and Systems for Video Technology, Vol. 11, no. 6, pp. 703-715, 2001.

[46] Li, C., Huang, Y., & Zhu, L. Color texture image retrieval based on Gaussian copula models of Gabor wavelets. Pattern Recognition, Vol. 64, pp. 118–129, 2017.

[47] T. Mäenpää, M. Pietikäinen , Classification with color and texture: jointly or separately? Pattern Recognit. Vol. 37 (8), pp.1629–1640, 2004.

[48] X. Qi, R. Xiao, C. Li, Y. Qiao, J. Guo, X. Tang, Pairwise rotation invariant cooccurrence local binary pattern, IEEE Trans. Pattern Anal. Mach. Intell. Vol. 36 (11), pp. 2199–2213, 2014.

[49] Liu, Guang-Hai Jing-Yu Yang, Content-based image retrieval using color difference histogram, Vol. 46, Issue 1, pp. 188-198, 2013.

[50] A. Hafiane, G. Seetharaman, B. Zavidovique, Median binary pattern for textures classification, in: Proceedings of the 4th International Conference on Image Analysis and Recognition, pp. 387–398, 2007.

[51] G-H Liu, J-Y Yang, Content-based image retrieval using color difference histogram, Pattern Recognit. Vol. 46 pp. 188–198, 2013.

[52] T. Deselaers, D. Keysers , H. Ney, Features for image retrieval: an experimental comparison, Inf. Retrieval Vol. 11 (2), pp. 77–107, 2008.

[53] J.Z. Wang, J. Li, G. Wiederhold, Simplicity: semantics-sensitive integrated matching for picture libraries, IEEE Trans. Pattern Anal. Mach. Intell. Vol. 23 (9), pp. 947–963, 2001.

[54] J. Han, K-K. Ma, Rotation-invariant and scale-invariant Gabor features for texture image retrieval, Image Vis. Comput. Vol. 25 (9), pp. 1474–1481, 2007.

[55] G-H Liu, Image Rank Machine Based on Visual Attention Mechanism <http:// www.ci.gxnu.edu.cn/cbir/Dataset.aspx>.